EasyChair Preprint

№ 2066

Dynamic modelling of a projectile launcher with controlled double inverted pendulum

Paras Savnani, Mihir Chauhan, Akash Mecwan and Rajesh Patel

December 1, 2019

Dynamic modelling of a projectile launcher with controlled double inverted pendulum

P. S. SAVNANI, M.M. CHAUHAN, A.I. MECWAN, R.N. PATEL

Institute of Technology, Nirma University, Ahmedabad-382481 Gujarat, India. Mihir.chauhan@nirmauni.ac.in

ABSTRACT: The aim of this paper is to form a mathematical model to simulate the dynamics of a unique mechanism which can be used in a projectile launching machine. This mechanism is a bi-linkage mechanism with two sets of pivots having rigid and flexible links respectively and the torque to drive the mechanism is applied at the first pivot via a pneumatic cylinder. The mathematical model of this system is derived assuming the system to be a controlled double inverted pendulum and the trajectory of the ball, resulting from the combined motion of the links, is assumed to follow circular path for a small segment. The launch parameters i.e. launch velocity and launch angle are derived from the numerical analysis of the mathematical model using simulation software and these parameters are experimentally verified to a great degree of accuracy.

KEYWORDS: Circular path, Controlled double inverted pendulum, Flexible link, Launch parameters, Mathematical model, Projectile launching machine.

1 INTRODUCTION

Projectile launchers have been a topic of research since the dawn of mankind. From toys to warfare siege machines, these mechanisms have been of great importance to us. From lever operated catapults (Rihll, 2007) to gun powder cannons (Dupuy & Nevitt, 1990), people use these machines to launch different projectiles. Most of these machines utilize the principle of mechanical advantage in their operation. Here, a unique bi-linkage mechanism is used to launch projectiles. Compared to conventional projectile launchers, this mechanism provides certain extra parameters to control the projectile's trajectory, thus it is very versatile.

The objective of this report is to establish a correlation between the system and the projectile's desired outcomes which include its range and height. This report tries to derive a mathematical model to predict the outcomes and the potency of the simulated results of the model are tested experimentally. The simulation is carried out using the 'OCTAVE' software and the experimental values are analysed in a video analysis software 'TRACKER'.

The mechanism is assumed to be a controlled double inverted pendulum (Zhong & Rock, 2001) as shown in Figure 1 and the mathematical model is generated on this hypothesis. A double inverted pendulum is a system having two pendulums attached end to end with each other and it exhibits periodic, quasi-periodic and chaotic behaviour (Rafat, Wheatland, & Bedding, 2009). Here, the first pendulum is a continuous mass system while the second pendulum is a lumped mass system. Double pendulum's motion is highly dynamic and nonlinear in nature (Ohlhoff & Richter, 2000), therefore its trajectory is difficult to predict. Here, Euler-Lagrange Equations (Morin, 2007) (Widnall, 2009) are used to derive the mathematical model of the dynamic system.

After, the mathematical model is derived in terms of second order differential equations (Hand & Finch, 1998) (Polking, Boggess, & Arnold, 2005), the software Octave is used for numerical simulation and to plot the trajectories and velocities of both links. Then, co-ordinate transformation of the trajectory points is done to coincide the assumed circle's centre with the origin and the instantaneous velocity and the launch angle at the desired point are found and these resultant parameters are used to predict the outcomes. Finally the theoretical values are compared with experimental values to check the accuracy of the mathematical model. The experimental setup is an autonomous machine designed on the basis of this mechanism, which can launch the projectiles at different input parameters thus facilitating in verification process.

2 MATHEMATICAL MODELLING

As shown in figure 1, the first link is an aluminium extrusion, which is rotated about a fixed pivot point and it is extended to apply an external force (F) on the link i.e. torque to the fixed pivot. The external force is applied

using a pressure filled pneumatic cylinder which is mounted on a rigid frame in the system. The second link is a string suspended ball which rotates about the detachable pivot point due to the torque applied at the fixed pivot point. The second link is detached once the launch angle is reached. The model is based on certain underlying assumptions. Here, the frictional forces are neglected in the model. Also, the suspended ball causes no air resistance. Apart from this, the first link is assumed to be rigid and is considered as a continuous mass system and the string in second link is non elastic and massless. The centre of mass of first link is midway between origin and the detachable pivot (i.e. distance d is very small compared to l_1). Also, it is assumed that the centre of mass of second link moves in a near circular trajectory for a small path.

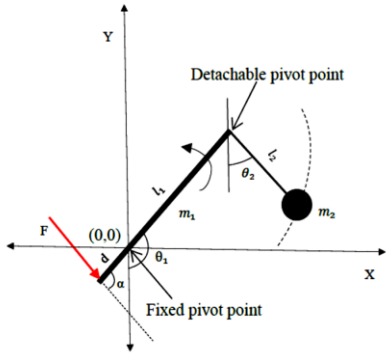

Figure 1.Double Inverted Pendulum Controlled Using an External Force

The dynamic modelling of the system is derived using the Lagrange formulation,

$$\frac{d}{dt}\left(\frac{\partial L}{\partial \dot{\theta}_i}\right) - \frac{\partial L}{\partial \theta_i} = \tau_i \quad (1)$$

Where, L = Lagrange function, θ_i = Generalized coordinate, τ_i=External Torque, i =1, 2

2.1 *Position of masses*

As shown in Figure 1, the centre of mass of first link lies at $\frac{l_1}{2}$ distance from origin and centre of mass of second link is at distance l_2 from detachable pivot, as string is considered as massless. The position vectors of centre of masses of first and second links are $\overrightarrow{r_1}$ and $\overrightarrow{r_2}$ respectively.

$$\overrightarrow{r_1} = \begin{bmatrix} \frac{l_1}{2}\sin(\theta_1) \\ -\frac{l_1}{2}\cos(\theta_1) \end{bmatrix} \quad \text{and} \quad \overrightarrow{r_2} = \begin{bmatrix} l_1 sin(\theta_1) + l_2 sin(\theta_2) \\ -l_1 cos(\theta_1) - l_2 cos(\theta_2) \end{bmatrix} \quad (2)$$

Differentiating and squaring the equations:

$$\left|\overrightarrow{r_1}\right|^2 = \left(\frac{l_1}{2}\right)^2 \dot{\theta_1}^2 \quad \text{and} \quad \left|\overrightarrow{r_2}\right|^2 = l_1^2\dot{\theta}_1^2 + l_2^2\dot{\theta}_2^2 + 2l_1l_2\dot{\theta}_1\dot{\theta}_2\cos(\theta_1 - \theta_2)) \quad (3)$$

2.2 *Energy Equations:*

The system has two different forms of energy: kinetic energy (the energy of motion) and potential energy. T_1 and T_2 are kinetic energies and V_1 and V_2 are potential energies for first and second links respectively. Kinetic energy for each link is the summation of translational and rotational energies and potential energy for each link is the potential energy of their centre of masses with respect to the origin.

$$T_i = \frac{1}{2}m_i\left|\vec{r_i}\right|^2 + \frac{1}{2}I_i\dot{\theta_i}^2 \quad \text{and} \quad V_i = m_i g y_i \quad (4)$$

Where, m_i = Mass of link, $\vec{r_i}$ = Position vector, I_i = Moment of Inertia, θ_i =Generalized coordinate, g=Gravitational Constant, y_i= y coordinate of centre of mass.

Substituting (2) and (3) in equation (4):

$$T_1 = \frac{1}{6}m_1l_1^2\dot{\theta}_1^2 \quad (5)$$

$$T_2 = \frac{1}{2}m_2(l_1^2\dot{\theta}_1^2 + l_2^2\dot{\theta}_2^2 + 2l_1l_2\dot{\theta}_1\dot{\theta}_2\cos(\theta_1 - \theta_2)) \quad (6)$$

$$V_1 = -m_1g(\tfrac{l_1}{2}\cos(\theta_1)) \quad (7)$$

$$V_2 = -m_2g(l_1\cos(\theta_1) + l_2\cos(\theta_2)) \quad (8)$$

2.3 *Lagrange function*

It is the difference of total kinetic energy and potential energy in the system. Following equation gives the Lagrangian:

$$L = T_1 + T_2 - (V_1 + V_2) \tag{9}$$

Substituting (5), (6), (7) and (8) in equation (9) and simplifying:

$$L = \left(\frac{1}{6}m_1 + \frac{1}{2}m_2\right) l_1{}^2\dot{\theta}_1{}^2 + \frac{1}{2}m_2 l_2{}^2\dot{\theta}_2{}^2 + m_2 l_1 l_2 \dot{\theta}_1\dot{\theta}_2\cos(\theta_1 - \theta_2) + (\frac{1}{2}m_1 + m_2)gl_1\cos(\theta_1) + m_2 g l_2\cos(\theta_2) \tag{10}$$

Differentiating equation (10) with respect to $\dot{\theta}_i$ and then differentiating the result with respect to time, also differentiating equation (10) with respect to θ_i and putting these values in equation (1) for i =1,2 respectively :

$$\left(\frac{1}{3}m_1 + m_2\right) l_1{}^2\ddot{\theta}_1 + m_2 l_1 l_2 \ddot{\theta}_2\cos(\theta_1 - \theta_2) - m_2 l_1 l_2 \dot{\theta}_2\sin(\theta_1 - \theta_2)(\dot{\theta}_1 - \dot{\theta}_2) + m_2 l_1 l_2 \dot{\theta}_1\dot{\theta}_2 \sin(\theta_1 - \theta_2) + (\frac{m_1}{2} + m_2)gl_1 \sin(\theta_1) = \tau_1 \tag{11}$$

$$m_2 l_2{}^2\ddot{\theta}_2 + m_2 l_1 l_2 \ddot{\theta}_1\cos(\theta_1 - \theta_2) - m_2 l_1 l_2 \dot{\theta}_1\sin(\theta_1 - \theta_2)(\dot{\theta}_1 - \dot{\theta}_2) - m_2 l_1 l_2 \dot{\theta}_1\dot{\theta}_2\sin(\theta_1 - \theta_2) + m_2 g\, l_2\sin(\theta_2) = \tau_2 \tag{12}$$

The torque (τ_1) in equation (11) can be determined using Figure 2, where F is the external force applied to the link at a distance 'd' from the origin. Here, 'φ' is the angle of piston with horizontal and 'α' is the angle of force with the link. And, 'b' is the distance of origin with X axis and cylinder's intersection.

$$\tau_1 = Fd\sin\alpha \qquad \text{and} \qquad F = \frac{P\pi D^2}{4} \tag{13}$$

Where, P = Pressure in pneumatic cylinder, D = Bore diameter of pneumatic cylinder

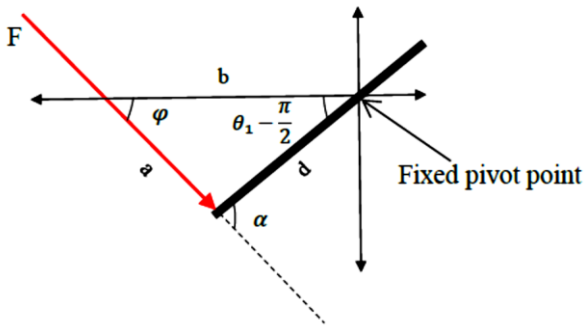

Figure 2. The force co-relation triangle

Using Figure 2,

$$b = d\cos\left(\theta_1 - \frac{\pi}{2}\right) + a\cos\varphi \quad \text{and} \quad a = -\left(\frac{d}{\sin\varphi}\right)\cos\theta_1 \tag{14}$$

$$\sin(\alpha) = \frac{b\sin\varphi}{d} \tag{15}$$

Substituting equation (14) in equation (15) and simplifying the equation:

$$\sin(\alpha) = \sin\theta_1\sin\varphi - \cos\theta_1\cos\varphi = -\cos(\theta_1 + \varphi) \tag{16}$$

Substituting equation (16) in (13),

$$\tau_1 = -Fd\cos(\theta_1 + \varphi) \tag{17}$$

Comparing equation (11) and (17) and solving for $\ddot{\theta}_1$,

$$\ddot{\theta}_1 = \frac{-m_2 l_2\ddot{\theta}_2\cos(\theta_1 - \theta_2) - m_2 l_2\dot{\theta}_2{}^2\sin(\theta_1 - \theta_2) - (\frac{m_1}{2} + m_2)g\sin(\theta_1) - \frac{F}{l_1}d\cos(\theta_1 + \varphi)}{\left(\frac{1}{3}m_1 + m_2\right)l_1} \tag{18}$$

The torque (τ_2) in equation (12) is zero, as no external torque is applied at the detachable pivot point. Substituting $\tau_2 = 0$ in equation (12) and solving for $\ddot{\theta}_2$,

$$\ddot{\theta}_2 = \frac{-l_1\ddot{\theta}_1\cos(\theta_1 - \theta_2) + l_1\dot{\theta}_1{}^2\sin(\theta_1 - \theta_2) - g\sin(\theta_2)}{l_2} \tag{19}$$

The equations (18) and (19) are coupled, therefore they are made independent in the following steps.

Using equations (18) and (19),

$$\ddot{\theta_1} = \frac{-m_2 l_1 \dot{\theta}_1^2 \sin(\theta_1 - \theta_2)\cos(\theta_1 - \theta_2) + m_2 g \sin(\theta_2)\cos(\theta_1 - \theta_2) - m_2 l_2 \dot{\theta}_2^2 \sin(\theta_1 - \theta_2) - (\frac{m_1}{2} + m_2) g \sin(\theta_1) - \frac{F}{l_1} d \cos(\theta_1 + \varphi)}{\left(\frac{1}{3}m_1 + m_2\right) l_1 - m_2 l_1 \cos^2(\theta_1 - \theta_2)} \quad (20)$$

and,

$$\ddot{\theta_2} = \frac{m_2 l_2 \dot{\theta}_2^2 \sin(\theta_1 - \theta_2)\cos(\theta_1 - \theta_2) + (\frac{m_1}{2} + m_2) g \sin(\theta_1)\cos(\theta_1 - \theta_2) + \frac{F}{l_1} d \cos(\theta^1 - \theta^2)\cos(\theta_1 + \varphi) + \left(\frac{1}{3}m_1 + m_2\right) l_1 \dot{\theta}_1^2 \sin(\theta_1 - \theta_2) - \left(\frac{1}{3}m_1 + m_2\right) g \sin(\theta_2)}{\left(\frac{1}{3}m_1 + m_2\right) l_2 - m_2 l_2 \cos^2(\theta_1 - \theta_2)} \quad (21)$$

Converting these second order differential equations into four first order differential equations using state space representation and solving using computer software, the solution of these equations at each time step within a defined time span is found. The observed time span decides the operating range of θ_1 and θ_2. The values of θ_1 and θ_2 are inserted in equation (2) to get the values of trajectory co-ordinates. Now the centre of mass of second link ($\overrightarrow{r_2}$) is assumed to move in a near circular trajectory for a small path as shown in Figure 3.

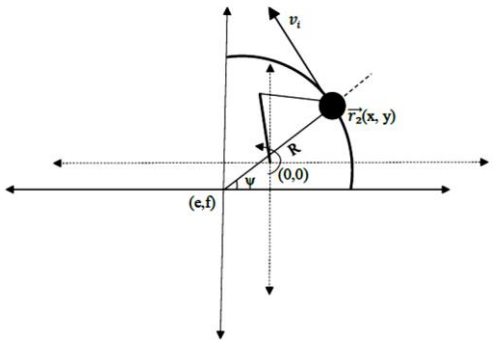

Figure 3. Coordinate transformation

Inputting the trajectory points of $\overrightarrow{r_2}$ in the equation of a general circle, the radius and the centre of the arc are found. Making the origin and centre of the circle coincident and transforming the trajectory coordinates, the values of ψ are found for each trajectory point as:

$$\psi = \tan^{-1}\left(\frac{\bar{y}}{\bar{x}}\right) = \tan^{-1}\left(\frac{y-f}{x-e}\right) \quad (22)$$

Here, $\bar{x}$ and $\bar{y}$ are transformed coordinate of arc, e and f are coordinate of centre point.

Plotting ψ vs t, the instantaneous slope at ψ_{final} is found, which will give $\dot{\psi}$.

Thus,

Final launch angle = $\theta = \frac{\pi}{2} - \psi_{final}$ and Final launch velocity = $v_i = R\dot{\psi}$ (23)

3 SIMULATION RESULTS AND EXPERIMENTAL VALIDATION

Here, the double inverted pendulum's trajectory is simulated using a computer program and finally the angles and velocities of both the links are plotted with respect to time. The simulation is carried out using the ordinary differential equations obtained in the mathematical model.

Table 1: Input parameters

m_1	0.4kg
m_2	0.1kg
l_1	0.57m
l_2	0.35m
g	$9.81\frac{m}{s^2}$
d	0.08m
P	$5.6*10^5$pascal
φ	27^0
t	0.5s
D	0.025m

Table 2: Initial Boundary Conditions

θ_1	125^0
θ_2	0^0
$\dot{\theta}_1$	0
$\dot{\theta}_2$	0

Here, the governing input parameters are Force (F), Length of first link (l_1) and Angle of first link (θ_1). Furthermore, the Force is dependent on other primary parameters like Pressure in cylinder (P), Bore diameter (D). Every other parameter (e.g. m_1, m_2, θ_2, d etc.) is fixed for the analysis. Table 1 shows a set of values for which the experiment was carried out and finally it is compared with the simulation results.

3.1 *Simulation results:*

To evaluate the performance of the system, the mathematical model is used to plot the positions of both links with respect to time. Initial angles of first link and second link are 125^0 and 0^0 respectively with vertical axis. The curves obtained are non-linear and without any periodicity. From figure 4, it is inferred that both the curves have increasing trends but the rate of increase of second link's angle is greater than the rate of increase in first link's angle. Here, the first link's final angle is constrained and the time it took to reach that angle is found. This time decides the launch position, angle and velocity of the projectile.

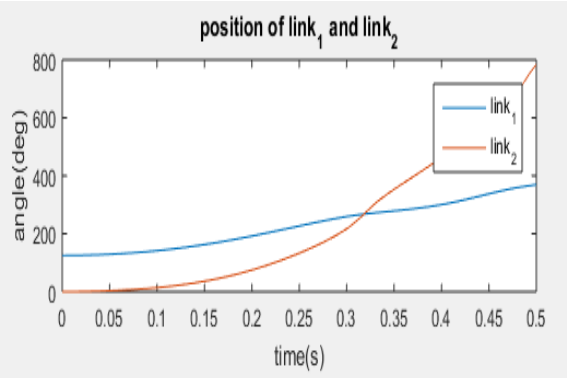

Figure 4. θ_1/θ_2 vs time

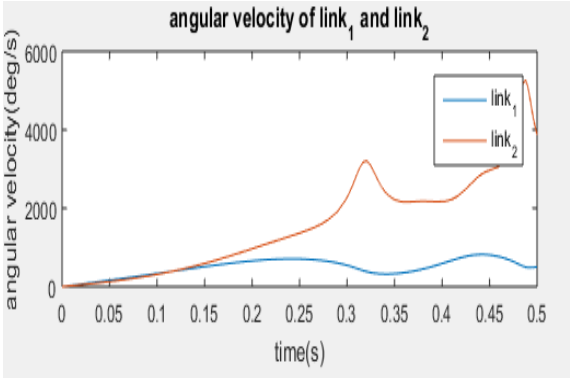

Figure 5. $\dot{\theta}_1/\dot{\theta}_2$ vs time

In Figure 5 the profile of angular velocity vs time of both links have a high degree of non-linearity. Here, the first link shows non-periodic oscillatory motion, while the second link shows a general increasing trend with one sided oscillations. Figure 6 shows the angle of projectile (centre of mass of second link) with horizontal axis after the coordinate transformation. The curve shows rapid increasing trend with time. This curve is derived from the projectile's trajectory using the transformed coordinates.

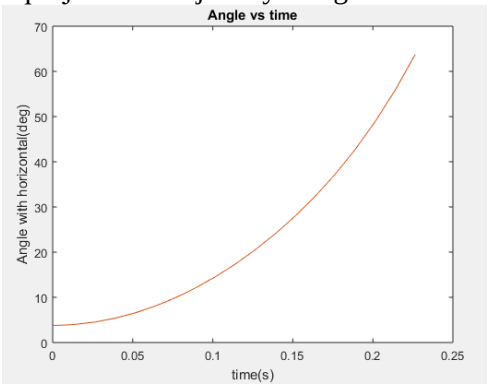

Figure 6. ψ vs time

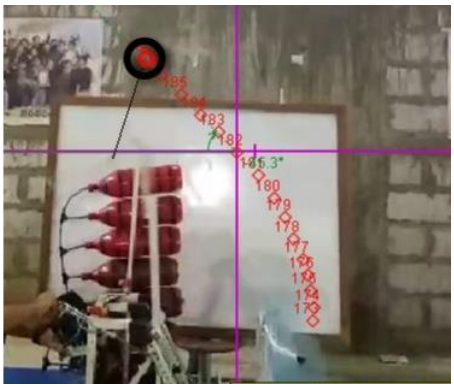

Figure 7. Actual trajectory of the projectile

The curve fitting tool is used to fit this curve into a four degree polynomial with R square value = 1 and RMSE = 0.0582. The analysed time span is less than 0.25 seconds because that is the experimental limit on the developed physical setup. Following equation is the result of curve fitting data:

$$\psi = p_1 t^4 + p_2 t^3 + p_3 t^2 + p_4 t^1 + p_5 t^0 \quad (24)$$

Here, $p_1 = 16620,\ p_2 = -5073, p_3 = 1530, p_4 = -14.34, p_5 = 1.824$

Substituting the value of time in this equation will give the angle (ψ) at required instant i.e. launch angle will be $\theta = \frac{\pi}{2} - \psi$.

As the limit for first link is 190^0, so from figure 4 the time required to reach this point is 0.198 seconds. Inputting this value in above equation yields $\psi = 45.12^0$, thus $\theta = 44.88^0$. And substituting the value of time in its

derivative will give the angular velocity at that instant i.e. launch velocity will be $v_i = R\dot{\psi}$. Inputting value of time yields, $\dot{\psi} = 510.935^0 s^{-1}$ or $8.91\frac{rad}{s}$ and R = 0.75m from circle's equation so $v_i = 6.68\frac{m}{s}$.

3.2 *Experimental validation*

The results from the dynamic model have been tested on a physical system within tolerable limits. The projectile launcher is built using a ISO 6432/ CETOP RP52P standard pneumatic cylinder having bore diameter 25mm and stroke length 125mm and a 5/2 solenoid to control its actuation .The first link is made of a hollow aluminium extrusion of cross section 22*22mm with thickness 1mm. The second link consists of a non-elastic thread and a rigid ball as the projectile at the end. The fixed pivot point has bearing support with two 8mm SKF bearings. The joint between first link and the second link is a detachable pin joint which is detached from the system, when the launch angle is reached.

Table 3: Comparison of simulation and experimental results

Output Parameters	Final Angle ($\theta = \frac{\pi}{2} - \psi$)	Final Velocity(v_i)
Simulation	44.88^0	$6.68\frac{m}{s}$
Experimentation	45.3^0	$6.59\frac{m}{s}$

Here, a video analysis software 'TRACKER' is used to record the actual trajectory of the projectile. The trajectory is divided into two phases i.e. when the projectile is attached with the system, in figure 7 from start of red marks to the intersection of magenta lines and after that. After the intersection point the projectile leaves the system and follows the projectile motion with the output parameters of the system i.e. angle and velocity. The actual trajectory matches with the simulation results and gives same output parameters as predicted by the mathematical model within tolerable limits. Thus, it is observed that the experimental values match with the simulation results within tolerable limits. The small variations can be attributed to the assumptions made in the mathematical model.

4 CONCLUSION

The system is analysed using a mathematical model derived using Lagrangian mechanics approach to the double inverted pendulum incorporating the dynamics of the system. Furthermore, the simulation results match with the experimental results thus, proving the applicability of this model. The equation obtained from the curve fitting data for the input parameters used in the simulation will vary with another set of data. As, this model predicts the trajectory and the launch parameters accurately, it has widespread applications in industrial launchers, weapons technology, sports training machines etc. The present model can be further extended by considering the frictional forces and air resistance to predict more realistic behaviour of the launching mechanism.

REFERENCES

Dupuy, & Nevitt, T. 1990. *The Evolution of Weapons and Warfare.* New York: Da Capo Press.

Hand, L. N., & Finch, J. D. 1998. *Analytical Mechanics.* NewYork: Cambridge University Press.

Morin, D. 2007. The Lagrangian Method. In *Introduction to Classical Mechanics, With Problemsand Solutions,* VI1 - VI55. Cambridge University Press.

Ohlhoff, A., & Richter, P. H. 2000. Forces in double pendulum. *Journal of Applied Mathematics and Mechanics, 80*(8).

Polking, J., Boggess, A., & Arnold, D. 2005. *Differential Equations with Boundary Value Problems.* New Jersey: Pearson Prentice Hall.

Rafat, M. Z., Wheatland, M. S., & Bedding, T. R. 2009;. Dynamics of a double pendulum with distributed mass. *American Journal of Physics*.

Rihll, T. E. 2007. *The Catapult: A History.* Yardley: Westholme Publishing.

Widnall, S. 2009. *LectureL20- EnergyMethods:Lagrange'sEquations.* MIT OpenCourseWare.

Zhong, W., & Rock, H. 2001. Energy and passivity based control of the double inverted pendulum on a cart. *Proceedings of the 2001 IEEE international Conference on Control Application,* 896-901. Mexico: IEEE.